Synthesis of conjugates of (a*R*,7*S*)-colchicine with monoterpenoids and investigation of their biological activity

*E. S. Shchegravina,[a] S. D. Usova,[a] D. S. Baev,[b] E. S. Mozhaitsev,[b] D. N. Shcherbakov,[c] S. V. Belenkaya,[c,d] E. A. Volosnikova,[c] V. Yu. Chirkova,[e] E. A. Sharlaeva,[e] E. V. Svirshchevskaya,[f] I. P. Fonareva,[a] A. R. Sitdikova,[a] N. F. Salakhutdinov,[b] O. I. Yarovaya,[b] and A. Yu. Fedorov[a]**

[a]*Lobachevsky State University of Nizhny Novgorod, k. 2, 23 prosp. Gagarina, 603950 Nizhny Novgorod, Russian Federation. E-mail: afedorovnn@yandex.ru*

[b]*N. N. Vorozhtsov Novosibirsk Institute of Organic Chemistry, Siberian Branch of the Russian Academy of Sciences, 9 prosp. Akad. Lavrent'eva, 630090 Novosibirsk, Russian Federation*

[c]*State Scientific Center of Virology and Biotechnology "Vector", 630559 Koltsovo, Novosibirsk Region, Russian Federation*

[d]*Novosibirsk State University, 1 ul. Pirogova, 630090 Novosibirsk, Russian Federation*

[e]*Altai State University, 61 Leninsky prosp., 656049 Barnaul, Russian Federation*

[f]*Department of Immunology, M. M. Shemyakin and Yu. A. Ovchinnikov Institute of Bioorganic Chemistry, Russian Academy of Sciences, 16/10 ul. Miklukho-Maklaya, 117997 Moscow, Russian Federation*

Conjugates of the natural alkaloid (a*R*,7*S*)-colchicine with bicyclic monoterpenoids and their derivatives were synthesized for the first time. Molecular docking of the synthesized agents in the active site of the main viral protease of the SARS-CoV-2 virus was carried out. The cytotoxic properties of the agents against different cell lines and the ability to inhibit the main viral protease 3CLPro were studied.

Key words: colchicine, monoterpenoids, SARS-Cov-2 3CLPro, molecular docking, antiproliferative activity.

The pandemic caused by the SARS-Cov-2 coronavirus, which has been going on for more than two years, is an acute medical and social problem. Despite a massive vaccination campaign that began in early 2021, many new cases of the disease are registered every day in many countries of the world, and the number of deaths over the entire period of the pandemic has exceeded 6 million.

The development of effective antiviral drugs requires a deep understanding of the mechanism of action of the virus on host cells. To date, the Food and Drug Administration (FDA) has approved only a few drugs for the treatment of SARS-Cov-2, and some of them are recommended for emergency use only. Such drugs are represented by nucleotide analogs remdesivir[1] and molnupiravir,[2] as well as by the 3CLPro protease inhibitor Paxlovid.[3] The most promising clinical candidates currently under trial are Favipiravir[4,5] and drugs based on antibodies blocking IL-6 receptors.[6—9] Since the clinical course of SARS-Cov-2 varies greatly depending on the strain of the virus and is characterized by a wide range of severe symptoms (multiple organ failure, acute respiratory distress syndrome, cytokine storm, bleeding disorders, *etc.*), there is no single treatment protocol that is effective in all cases. Most protocols are aimed at preventing an uncontrolled reaction of the immune system.

* Fedorov Aleksey Yuryevich, born in 1971, Head of the Department of Organic Chemistry of the Faculty of Chemistry of the National Research Lobachevsky State University of Nizhny Novgorod (Nizhny Novgorod), Doctor of Chemical Sciences, Professor of the Russian Academy of Sciences (since 2018). He was elected a corresponding member of the Russian Academy of Sciences in 2022 (more information in *Russ. Chem. Bull.*, 2022, **71**, 1559; DOI: 10.1007/s11172-022-3565-4).

Published in Russian in *Izvestiya Akademii Nauk. Seriya Khimicheskaya,* Vol. 72, No. 1, pp. 248—262, January, 2023.

1066-5285/23/7201-0248 © 2023 Springer Science+Business Media LLC

Colchicine **1**, a natural alkaloid that interacts with microtubules of the cytoskeleton and is a known immunosuppressant, was considered as a promising drug for the treatment of Covid-19.[10—15] The ability of colchicine **1** and its derivatives to bind to tubulin and disrupt microtubule dynamics[16—20] causes destruction of the NLRP3 inflammasome receptor,[21] blocks cellular transport and cytokine infiltration,[22] and inhibits neutrophil activation. Suppression of neutrophil transport from capillaries to the focus of pathology is one of the key factors for reducing the inflammatory response. These properties of colchicine **1** may be useful in preventing massive infiltration of cytokines into lung tissue, which is often observed in severe cases of Covid-19.[23] Along with the pronounced anti-inflammatory effect, colchicine **1** is also able to exhibit inhibitory activity against the replication of certain viruses, such as Zika and dengue viruses.[24]

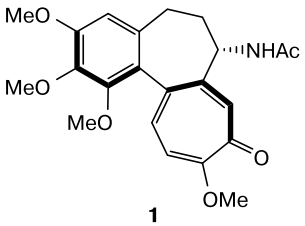

1

Another strategy for the treatment of Covid-19, along with the suppression of the excessive reaction of the immune system, is to inhibit the penetration of the virus into the host cells, to disrupt its replication and maturation processes. Due to the wide spectrum of biological activity, natural terpenoids and their synthetic analogs[25—29] can be considered as potential inhibitors of viral replication. Thus, borneol and camphor derivatives **2—4** demonstrate antiviral activity against Ebola,[30] Marburg,[31,32] and influenza[33] viruses. Non-polar scaffold structures in these compounds can interact with hemagglutinin and M2 ion channels, stabilizing the inactive conformation of these proteins,[34] thereby preventing the penetration of the virus into the cell. The activity of terpenoids against SARS-Cov-2 proteins,

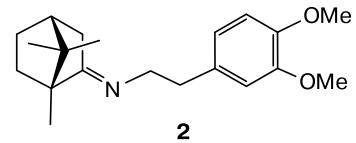

2

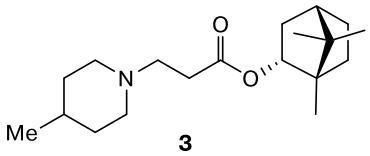

3

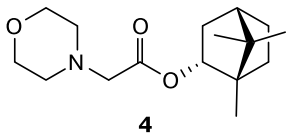

4

in particular, to the receptor-binding domain of the S-protein[35] and the 3CLpro protease, is being studied.[36,37]

The strategy of combination of active pharmacophore units in one molecule has been successfully implemented to obtain drugs against HIV,[38] influenza virus,[39] and Hantaan virus.[40] In the present work, conjugates of colchicine with various monoterpenoids were synthesized to study the possibility of their use as inhibitors of the main protease of SARS-Cov-2 (3CLPro).

Results and Discussion

Synthesis of target compounds. The molecular structure of the target conjugates is shown schematically in Fig. 1. The molecules of the target conjugates contain two active fragments: a colchicinoid that binds to the tubulin heterodimer and a terpenoid[33,41] that is potentially capable of interacting with viral proteins. Since the active parts of the molecules are aimed at different targets, the linker between them must contain a biocleavable bond. Terpenoids and their derivatives **5—10** were chosen for the synthesis of target conjugates.

To obtain target derivatives, deacetylcolchicine **13** was used as the starting compound, which was

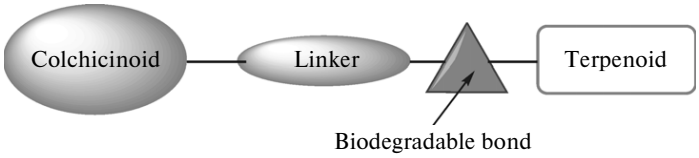

Fig. 1. Combination of pharmacophore blocks in the molecules of target conjugates of colchicine with monoterpenoids.

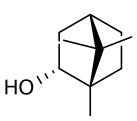

5 ((–)-Borneol)

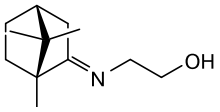

6 ((+)-Camphecene)

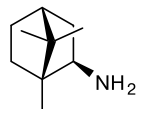

7 ((+)-Isobornylamine)

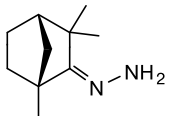

8 ((–)-Fenchone hydrazone)

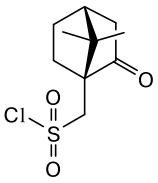

9 ((+)-10-Camphorsulfonyl chloride)

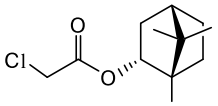

10 ((–)-Borneol chloroacetate)

synthesized from colchicine **1** in three steps (Scheme 1) according to modified known procedures.[42,43] At the first step, a protective *tert*-butoxycarbonyl group was introduced in colchicine **1**, which gave compound **11**. At the second step, the acetyl group was removed by the action of MeONa. At the third step, the Boc group in compound **12** was removed in an acid medium. Deacetylcolchicine **13** was obtained in 73% yield for three steps.

For conjugation with terpenoids, we synthesized derivatives of deacetylcolchicine **13** with glutaric anhydride and aminocaproic acid, compounds **14** and **15** (Scheme 2). The carboxylate derivative **14**, obtained in yield 45%, was used for conjugation with (–)-borneol **5** and (+)-camphecene **6** under the Yamaguchi esterification conditions, as well as with (+)-isobornylamine **7** and (–)-fenchone hydrazone **8** under the Steglich amidation conditions. As a result, derivatives **16**—**19** were synthesized in 69—83% yields. Amino derivative **15** was reacted with (+)-10-camphorsulfonyl chloride **9** and (–)-borneol chloroacetate **10**, which gave conjugates **20** and **21** in relatively low yields.

Molecular docking. Currently, an active search for possible inhibitors of the main protease of SARS-CoV-2 is under way. Since the conjugates synthesized in this work do not contain functional groups and unsaturated bonds capable of covalent interaction with the SH group of the catalytic amino acid residue Cys145, we focused on the search for possible non-covalent interactions. Earlier, among compounds of various chemical classes, there were found molecules that can inhibit the main protease of SARS-CoV-2 due to non-covalent interactions in its active site.[44—48] One of these compounds, namely ML188, was taken by us for comparison in calculations.

Carrying out the evaluation function of molecular docking IFD and calculating the free energy of

Scheme 1

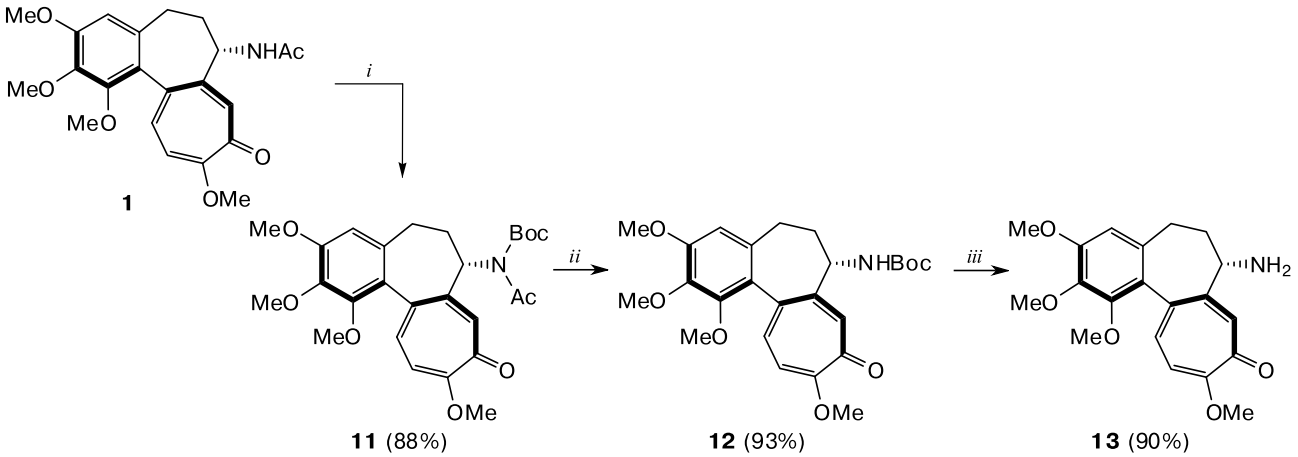

Reagents and conditions: *i.* Boc_2O, DMAP, Et_3N, MeCN, 100 °C, 3 h; *ii.* MeONa, MeOH, 40 °C, 2 h; *iii.* TFA, CH_2Cl_2, ~20 °C, 3 h.

Scheme 2

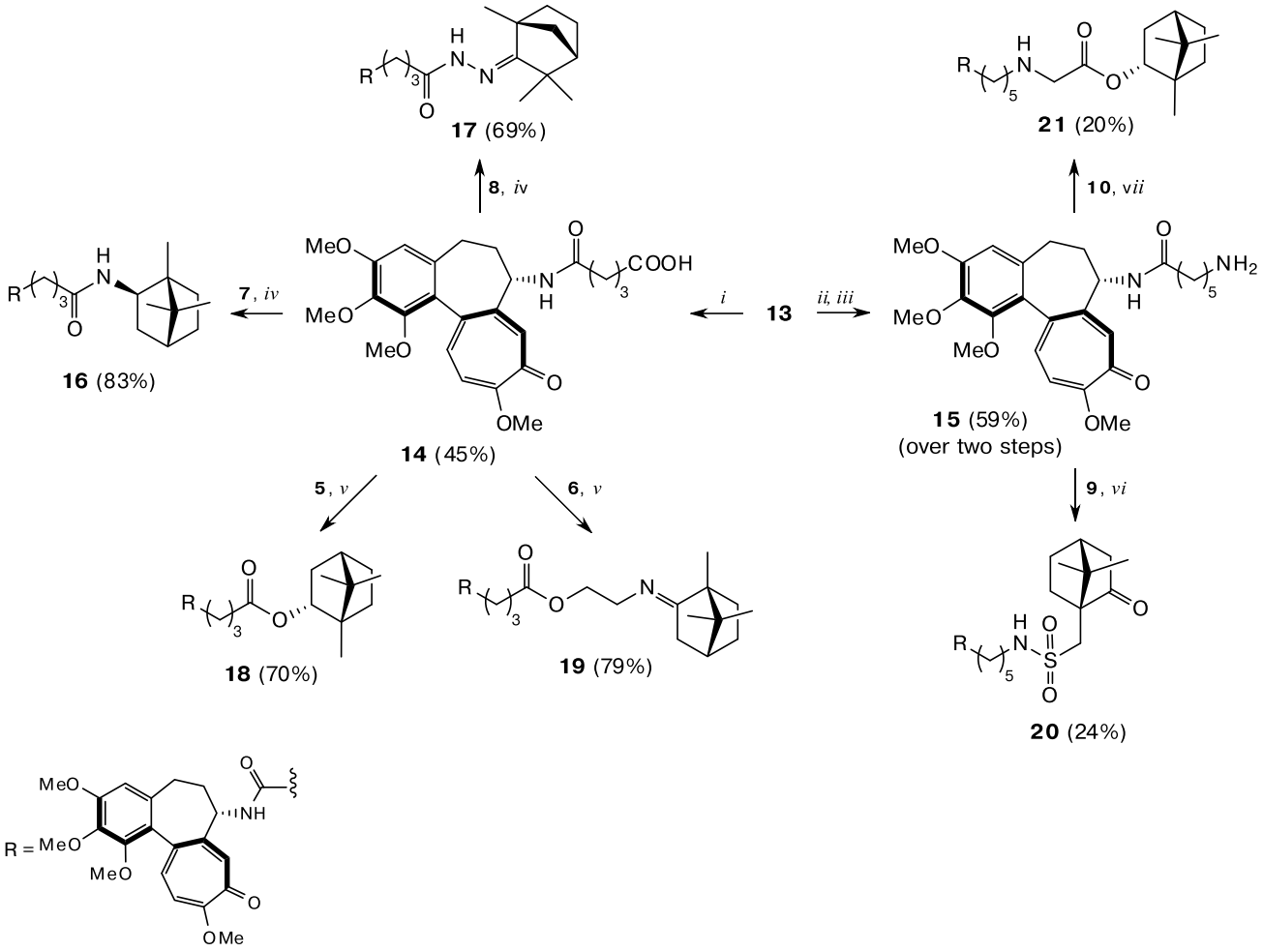

Reagents and conditions: *i*. glutaric anhydride, *N*-methylmorpholine (NMM), DMSO, 50 °C, 1 h; *ii*. *tert*-butyloxycarbonyl-6-aminohexanoic acid, diisopropylcarbodiimide (DIC), *N*-hydroxysuccinimide (NHS), $CHCl_3$, ~20 °C, 20 h; *iii*. TFA, CH_2Cl_2, ~20 °C, 1.5 h; *iv*. EDC·HCl, DMAP, CH_2Cl_2, ~20 °C, 16 h; *v*. 2,4,6-trichlorobenzoyl chloride (TCBC), Et_3N, DMAP, CH_2Cl_2, ~20 °C, 24 h; *vi*. DMAP, MeCN, 0 °C→~20 °C, 20 h; *vii*. Et_3N, CH_2Cl_2, ~20 °C, 16 h.

ligand—receptor complexes based on the principles of molecular mechanics and the generalized implicit Born solvation model (MM/GBSA) resulted in the data presented in Table 1. The method of semiempirical quantum mechanics (SQM) with parametrized models takes into account quantum mechanical effects and electronic properties in the study of protein—ligand interaction, which can improve the accuracy of the corresponding calculations.[49,50] In this regard, we optimized the ligand—receptor complexes obtained after performing molecular docking according to the IFD protocol using the semiempirical quantum mechanical (SQM) method PM6-D3H4 in combination with the COSMO implicit solvent model.

Molecular docking, which takes into account the flexibility of the side chains of amino acid residues of the main protease binding site, showed that the new colchicine monoterpene conjugates can exhibit significantly lower estimated binding energies compared to the non-covalent inhibitor ML188. In general, the chemical modification of colchicine **1** (−8.08 kcal mol^{-1}) leading to its conjugates with monoterpenes significantly increases the potential affinity for the binding site of the main protease. Deacetylation of colchicine **1** leads to a significant decrease in the potential affinity of deacetylcolchicine **13** (−6.9 kcal mol^{-1}). Molecular mechanics calculations of the free energy of ligand—receptor complexes show a similar trend. The free energy calcul-

Table 1. Calculated energies of protein—ligand interaction (E_{bond}) for the synthesized compounds

Compound	$-E_{bond}$/kcal mol^{-1}		
	IFD	MM/GBSA	SQM
1	8.08	65.14	42.28
6	4.93	41.26	18.63
13	6.90	43.21	37.98
16	9.83	83.17	36.21
17	9.08	85.88	68.26
18	9.93	89.92	44.67
19	8.66	90.50	38.29
20	11.11	88.11	34.92
21	10.25	89.03	54.92
ML188	8.43	81.77	61.38

ated by the MM/GBSA method for all complexes of the new conjugates and the main protease is below –80 kcal mol^{-1}, while the free energy of the complexes of colchicine **1** (–65.14 kcal mol^{-1}) and its deacetylated derivative **13** (–43.21 kcal mol^{-1}) with the protease is significantly higher than that of the conjugates and the non-covalent inhibitor ML188. The optimization of the conformations of the structures obtained by molecular docking and a more accurate estimate of the free energy carried out using a semi-empirical quantum chemical calculations gave smaller differences between the interaction energies of the conjugates **16**, **18**, **19**, and **20** compared to colchicine **1** and deacetylcolchicine **13**. The energies of conjugates **17** (–68.26 kcal mol^{-1}) and **21** (–54.92 kcal mol^{-1}) are comparable to the energy of inhibitor ML188 (–61.38 kcal mol^{-1}), so compounds **17** and **21** may be affinic for the main protease binding site.

Given these calculated results, it was important to study the conformations and features of non-covalent interactions of compounds in the active site of the main protease in comparison with the inhibitor ML188 (Fig. 2). The active site of the main protease is formed by dynamic loop structures containing two basic catalytic amino acid residues His41

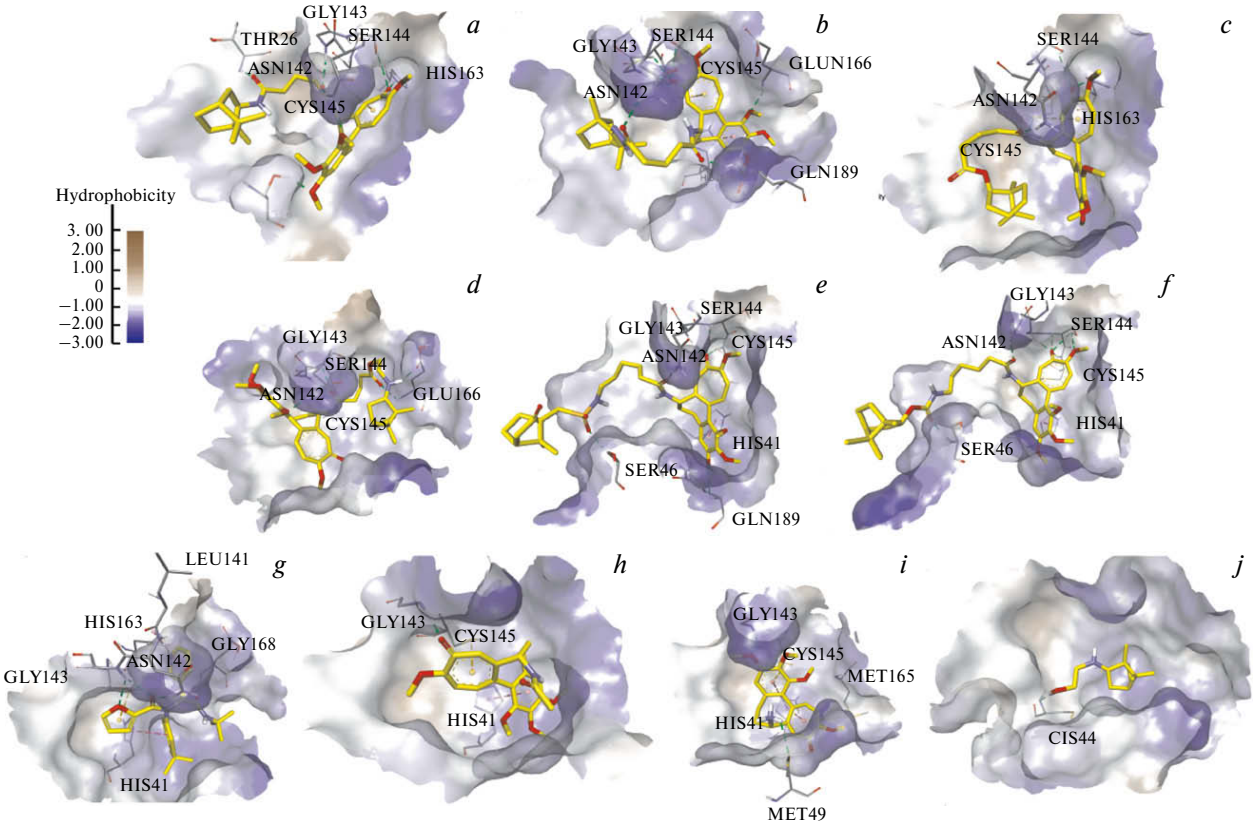

Fig. 2. Features of the location and non-covalent interactions of new conjugates of colchicine and monoterpenes **16** (*a*), **17** (*b*), **18** (*c*), **19** (*d*), **20** (*e*), and **21** (*f*) in the binding site of the main protease of SARS-CoV-2 in comparison with ML188 (*g*), colchicine **1** (*h*), deacetylcolchicine **13** (*i*), and camphecene **6** (*j*). Non-covalent interactions are shown by dotted lines: hydrogen bonds are in green, stacking interactions are in purple, interactions with the sulfur atom are in yellow, hydrophobic interactions are not shown.

and Cys145.[47] Stabilization of the loop structures, as well as interaction with His41 and Cys145 residues determine the activity of known inhibitors. The most favorable conformations of new conjugates obtained by molecular docking are characterized by the location of the colchicine scaffold in the active center of the main protease. The exception is compound **19** with its terpene scaffold being located in the active site of the enzyme. The carbonyl and methoxy groups in the tropolone ring of other conjugates, as well as the oxygen atom of the amide group, actively interact with amino acid residues in the 141—145 chain region, forming hydrogen bonds. The hydrogen bond acceptors in the inhibitor ML188 act similarly (oxygen atoms in the furan and amide fragments). Interestingly, the six-membered π-system of the colchicine scaffold of conjugates **16**, **20**, and **21** acts similarly to the phenyl ring of ML188, participating in the stacking interactions with the π-system of His41. Colchicine **1** and deacetylcolchicine **13** may be involved in the same stacking interaction. The π-systems of the tropolone ring of conjugates **16**, **17**, and **18**, are likely to interact with the sulfur atom of the catalytic amino acid residue Cys145.

To determine the stability of the ligand—protein complexes obtained by molecular docking according to the IFD protocol, the possible trajectories of the complexes over a period of 100 ns were studied by molecular dynamics. The root-mean-square deviation (RMSD) of the coordinates of the ligand atoms from the zero point of the simulation was calculated for each ligand during the simulation (Fig. 3). A significant contribution to the change in the RMSD is made by the general movement of the molecule of the SARS-CoV-2 main protease in the system. This is consistent with the data on the high flexibility and conformational mobility of proteases. Visual analysis of the trajectory of ligand—protein complexes allows one to determine the retention time of the ligand in the active site of the main protease of SARS-CoV-2 (Table 2).

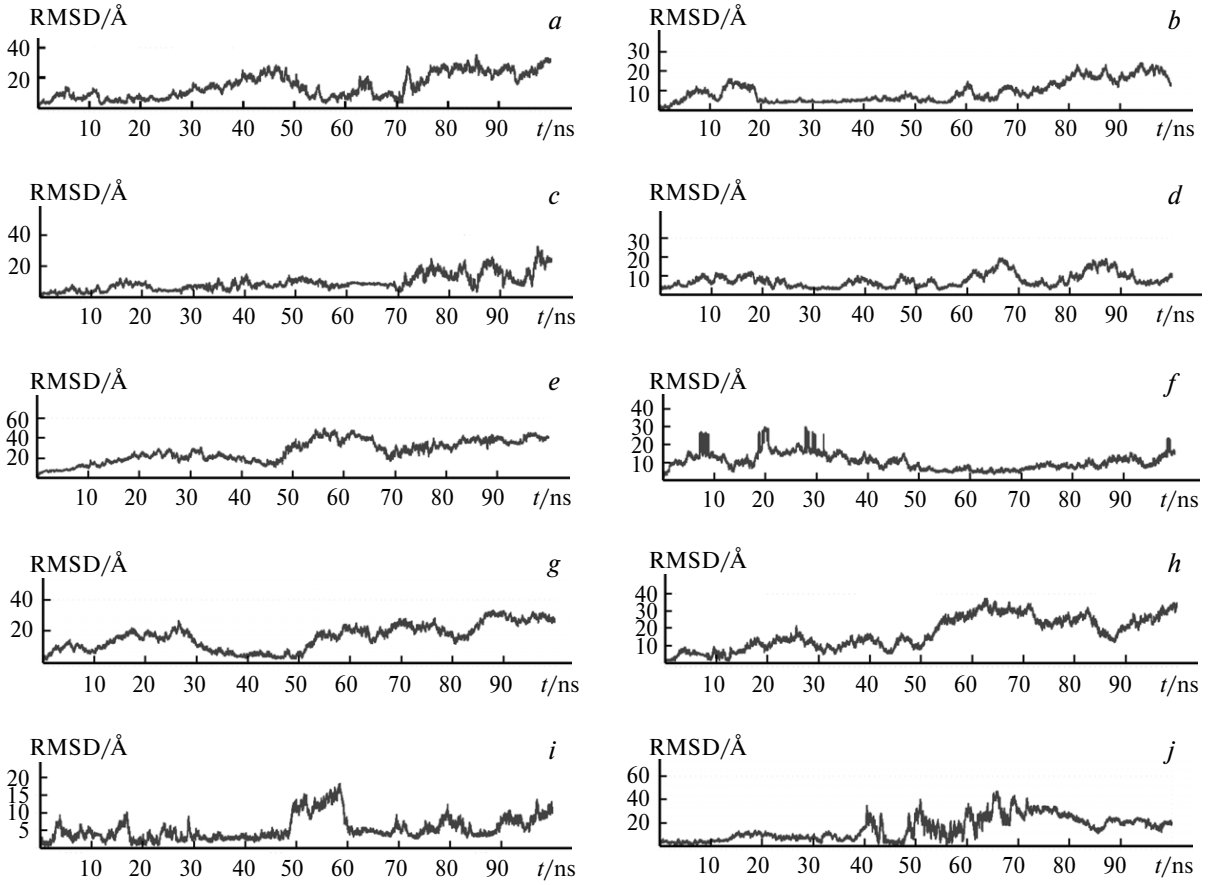

Fig. 3. Dependencies of the root-mean-square deviation (RMSD) of atomic coordinates of new conjugates of colchicine and monoterpenes **16** (*a*), **17** (*b*), **18** (*c*), **19** (*d*), **20** (*e*), and **21** (*f*) in the active site of the main protease of SARS-CoV-2 on the time of the molecular dynamics study (*t*) in comparison with inhibitor ML188 (*g*), colchicine **1** (*h*), deacetylcolchicine **13** (*i*), and camphecene **6** (*j*).

Table 2. Retention time (τ) of the ligand in the active site of the main protease of SARS-CoV-2

Compound	τ/ns
1	53
6	40
13	>100
16	41
17	>100
18	84.5
19	>100
20	48.0
21	>100
ML188	68

As the most stable ligands, one should consider not only compounds with the maximum retention time, but also those compounds that are subject to minimal fluctuations near the active site of the main protease. Deacetylcolchicine **13** demonstrates the most stable behavior. The change in its RMSD does not exceed 13 Å during the entire process of molecular dynamics simulation. In the period from 48 to 60 ns, the molecule of deacetylcolchicine **13** experienced fluctuations that did not lead to its exit from the active site. Interestingly, the inhibitor ML188 is subject to fairly strong fluctuations in the active site of the main protease, but exhibits a stable behavior over the simulation interval from 34 to 52 ns. The total retention time of compound ML188 in the active site is 68 ns, which is an average value among the molecules under consideration. Compounds **17** and **19** are the most stable among the new conjugates: they remained in the active site of the main protease throughout the entire simulation period and showed minimal fluctuations. Thus, the RMSD of conjugate **17** during the simulation period from 0 to 80 ns did not exceed 16 Å, while that of conjugate **19** did not exceed 11 Å during the simulation period from 0 to 60 ns. Compound **21**, although remained in the active site of the main protease throughout the simulation, experienced strong fluctuations at the initial step of the simulation, from 0 to 47 ns. Compound **16** was unstably bound in the active site of the main protease and was retained there for the shortest time (41 ns) among all conjugates. Conjugate **18** remained fairly stable during the entire retention time in the active site. Its RMSD during the period from 0 to 72 ns did not exceed 15 Å. Conjugate **20** showed instability in the active site of the main protease and was retained there for only 48 ns. A small molecule of camphecene **6** is quite stable in the active site of the main protease, but rapidly leaves it after 40 ns of molecular dynamics simulation. Colchicine **1** exhibits an unstable binding pattern in the active site of the main protease, leaving it after 53 ns.

Biological studies. The cytotoxic activity of all compounds obtained was studied against the cell lines of human adenocarcinoma (Colo-357), mouse mastocytoma (P815), mouse colon adenocarcinoma (CT-26), human embryonic renal epithelium (HEK-293), and Burkitt′s lymphoma (Raji) using a standard tetrazolium (MTT) test. The cells were incubated with test compounds for 72 h and the decrease in proliferation was measured, using colchicine **1** as a control compound. The results are presented in Table 3.

All compounds studied, except for colchicine **1**, exhibit antiproliferative activity in the micro- and submicromolar range of concentrations. A slight increase in antiproliferative activity is observed against Raji, P815, and HEK-293 cells. A significant decrease in the activity of conjugates **16**—**21** compared to colchicine is probably due to the presence of a bulky hydrophobic terpenoid fragment, which does not allow the colchicine fragment to interact with the active site of tubulin, which is located far enough from the protein surface. Among the target conjugates, compounds **20** and **21** showed the lowest activity, which is apparently explained by the increased hydrolytic stability of the sulfonamide and carbamate bonds present in these compounds. In general, all target conjugates possess moderate cytotoxicity, which allows them to be considered as potential antiviral agents.

Table 3. Antiproliferative activity of colchicine **1** and its conjugates with monoterpenoids **16**—**21**

Compound	IC_{50}*/nmol L^{-1}				
	Colo-357	CT-26	Raji	P815	HEK-293
1	4	12	0.2	21	6
16	4227	821	161	159	166
17	4197	873	129	174	158
18	3985	3867	749	884	836
19	4063	3954	846	823	890
20	5298	4872	973	879	901
21	4783	4977	938	921	946

* The results are presented as average values for five experiments. The standard deviation does not exceed 10% and is omitted for the sake of clarity.

Further, all synthesized compounds **16**—**21**, as well as colchicine **1**, deacetylcolchicine **13**, and camphecene **6** were tested for the ability to inhibit the main viral protease 3CLPro using a surrogate model we developed earlier.[51] The analysis is based on the measurement of the level of fluorescence, which increases due to the proteolytic degradation of the peptide substrate, which includes the 3CL-sensitive region of the SARS-CoV-2 polyprotein. The peptide fluorogenic substrate DabcylKTSAVLQ↓SGFRKME(Edans)NH_2 contains two fluorescent dyes, selected in such a way as to realize the FRET effect (FRET is the fluorescent resonance energy transfer). Degradation of the fluorogenic substrate suppresses the quenching of the donor dye fluorescence and promotes the appearance of longer wavelength fluorescence of the acceptor dye. The addition of the test compounds to this system allows one to assess the degree of enzyme inhibition by changing the intensity of the increase in fluorescence. The IC_{50} value was taken to be such a concentration of the studied compound that reduces the fluorescence level by 50% of the maximum observed in the absence of the inhibitor. Unfortunately, all the test compounds, except for conjugate **20** containing a fragment of 10-camphorosulfonic acid, turned out to be inactive. The known[52] protease inhibitors, such as ML188 and disulfiram, whose half-maximal inhibitory concentration values IC_{50} are equal to 1.56±0.55 and 6.25±1.97 μmol L^{-1}, respectively, were used as reference drugs. The IC_{50} value of compound **20** we determined in this work was 100±5.7 μmol L^{-1}. The changes in fluorescence per second from the concentration of inhibitor **20** are given in Table 4.

Table 4. Change in fluorescence intensity (ΔI^{fl}) of compound **20** depending on its concentration (C)

C/μmol L^{-1}	$\Delta I^{fl}/s^{-1}$
0	396.72
3.125	381.48
6.25	313.71
12.5	293.81
25	253.79
50	234.25
100	177.35
200	109.75
400	51.19

Despite the low activity against the main viral protease, the results of molecular docking and biological studies lead to a conclusion that the colchicine conjugates with monoterpenoid fragments are significantly less toxic against cancer cell lines than unmodified colchicine. Obviously, molecular docking without the use of biological studies does not allow one to draw an unambiguous conclusion about the presence of the target biological activity. The method used in this work for the synthesis of new compounds containing various pharmacophore fragments is of considerable interest from the point of view of medicinal chemistry and allows us to plan further synthesis of new compounds in order to search for efficient inhibitors of viral protease.

Experimental

^1H and ^{13}C NMR spectra were recorded in DMSO-d_6 on an Agilent DD2 400 spectrometer at 25 °C using Me_4Si as an internal standard. Mass spectra were recorded on a DSQ II mass spectrometer (Thermo Electron Corporation) with a quadrupole mass analyzer. Elemental analysis was performed on an Elementar instrument (Vario Micro Cube), all compounds were >95% pure. Column chromatography was performed using Merck Kieselgel 60 silica gel (70—230 mesh). All reactions were carried out using commercially available reagents. Solvents were purified according to standard procedures. Petroleum ether with b.p. 40—70 °C was used.

(*S*)-*tert*-Butyl[acetyl(1,2,3,10-tetramethoxy-9-oxo-5,6,7,9-tetrahydrobenzo[*a*]heptalen-7-yl)]carbamate (11). One half of a solution of di-*tert*-butyl dicarbonate (Boc_2O) (7.52 g, 34.5 mmol, 4.60 equiv.) in acetonitrile (8.00 mL) and triethylamine (2.10 mL) was added to a mixture of colchicine **1** (3.00 g, 7.51 mmol, 1.00 equiv.) and dimethylaminopyridine (915.00 mg, 7.50 mmol, 1.00 equiv.) in anhydrous acetonitrile (30.0 mL) under an inert atmosphere. The mixture was stirred for 1 h at 100 °C, followed by the addition of the second part of the Boc_2O solution. The mixture was stirred for 2 h at 100 °C, cooled to room temperature, volatiles were removed under reduced pressure. The target *N*-Boc-colchicine **11** was purified by column chromatography (eluent ethyl acetate—acetone (4 : 1)), the yield was 3.29 g (88%). M.p. 105 °C. ^1H NMR, δ: 7.27 (s, 1 H, H(8)); 7.11 (d, 1 H, H(11), J = 10.7 Hz); 7.02 (d, 1 H, H(12), J = 10.7 Hz); 6.77 (s, 1 H, H(4)); 4.90 (dd, 1 H, H(7), J = 12.3 Hz, J = 5.8 Hz); 3.87 (s, 3 H, OCH_3); 3.83 (s, 3 H, OCH_3); 3.77 (s, 3 H, OCH_3); 3.54 (s, 3 H, OCH_3); 2.69 (dd, 2 H, H(6), J = 13.5 Hz, J = 6.0 Hz); 2.33—2.26 (m, 1 H, H(5)); 2.23 (s, 3 H, $NC(O)CH_3$); 1.96—1.85 (m, 1 H, H(5)); 1.49 (s, 9 H, $NC(O)OC(CH_3)_3$). ^{13}C NMR, δ: 178.31, 170.79, 163.95, 153.55, 153.43,

150.91, 148.69, 141.26, 135.20, 134.96, 134.28, 132.16, 126.03, 112.59, 108.15, 84.80, 61.27, 61.09, 60.20, 56.48, 56.27, 32.24, 29.68, 27.72. MS (70 eV), *m/z* (I_{rel} (%)): 499 (2), 399 (40), 371 (16), 340 (18), 328 (26), 312 (82), 311 (46), 281 (62), 280 (40), 254 (34), 239 (19), 195 (18), 181 (15).

(*S*)-*tert*-Butyl(1,2,3,10-tetramethoxy-9-oxo-5,6,7,9-tetrahydrobenzo[*a*]heptalen-7-yl)carbamate (12). Derivative **11** (3.29 g, 6.60 mmol, 1.00 equiv.) and sodium methoxide (1.43 g, 26.4 mmol, 4.00 equiv.) were placed into a Schlenk flask and filled it with argon. Anhydrous methanol (34.0 mL) was added, the resulting solution was stirred for 2 h at 40 °C, neutralized with a saturated solution of NH_4Cl, and extracted with ethyl acetate (3×60 mL). The combined organic layer was dried with Na_2SO_4, the solvent was evaporated under reduced pressure. The resulting compound **12** was used in the next step without further purification. The yield was 2.79 g (93%); light orange crystals. M.p. 154 °C. ^{1}H NMR, δ: 7.69 (d, 1 H, NH, J = 7.8 Hz); 7.21 (s, 1 H, H(8)); 7.10 (d, 1 H, H(11), J = 10.6 Hz); 7.02 (d, 1 H, H(12), J = 10.8 Hz); 6.76 (s, 1 H, H(4)); 4.11—4.05 (m, 1 H, H(7)); 3.87 (s, 3 H, OCH_3); 3.83 (s, 3 H, OCH_3); 3.79 (s, 3 H, OCH_3); 3.54 (s, 3 H, OCH_3); 2.55 (dd, 1 H, H(6), J = 13.2 Hz, J = 5.9 Hz); 2.17 (td, 1 H, H(6), J = 13.0 Hz, J = 6.9 Hz); 2.04—1.95 (m, 1 H, H(5)); 1.86—1.77 (m, 1 H, H(5)); 1.32 (s, 9 H, $NC(O)OC(CH_3)_3$). ^{13}C NMR, δ: 178.00, 163.50, 154.50, 152.94, 151.03, 150.36, 140.69, 135.10, 134.39, 134.26, 130.51, 125.31, 112.12, 107.65, 60.83, 60.64, 56.01, 55.84, 54.90, 52.87, 40.78, 35.80, 28.14. MS (70 eV), *m/z* (I_{rel} (%)): 457 (2), 401 (33), 373 (67), 339 (23), 312 (80), 297 (96), 281 (100), 266 (57), 254 (48), 224 (35), 211 (50), 181 (42), 153 (48), 152 (62), 141 (33).

(*S*)-7-Amino-1,2,3,10-tetramethoxy-6,7-dihydrobenzo-[*a*]heptalen-9(5*H*)-one (13). Trifluoroacetic acid (7.00 mL) was added to a solution of derivative **12** (2.79 g, 6.14 mmol, 1.00 equiv.) in CH_2Cl_2 (30.0 mL) and the mixture was stirred for 3 h at room temperature, the acid was neutralized with aqueous $NaHCO_3$, and the solution was extracted with CH_2Cl_2 (3×50 mL). The combined organic layer was washed with brine and dried with Na_2SO_4, the solvent was evaporated under reduced pressure to afford deacetylcolchicine **13** (1.97 g, 90%) as yellow crystals. M.p. 137 °C. ^{1}H NMR, δ: 7.64 (s, 1 H, H(8)); 7.05 (d, 1 H, H(11), J = 10.6 Hz); 6.99 (d, 1 H, H(12), J = 10.8 Hz); 6.74 (s, 1 H, H(4)); 3.86 (s, 3 H, OCH_3); 3.83 (s, 3 H, OCH_3); 3.76 (s, 3 H, OCH_3); 3.55 (s, 3 H, OCH_3); 3.45 (dd, 1 H, H(6), J = 10.4 Hz, J = 5.9 Hz); 2.14 (m, 3 H, H(6), H(5)); 1.49 (td, 1 H, H(5), J = 10.0 Hz, J = 4.8 Hz). ^{13}C NMR, δ: 178.20, 163.26, 153.82, 152.73, 150.15, 140.47, 135.68, 134.88, 133.76, 131.83, 125.40, 111.84, 107.34, 60.66, 60.53, 55.90, 55.84, 53.11, 39.64, 29.87. MS (70 eV), *m/z* (I_{rel} (%)): 357 (50), 328 (18), 312 (64), 298 (100), 297 (64), 281 (43), 267 (30), 254 (36), 253 (18), 239 (16), 195 (14), 181 (20), 149 (19).

(*S*)-5-Oxo-5-[(1,2,3,10-tetramethoxy-9-oxo-5,6,7,9-tetrahydrobenzo[*a*]heptalen-7-yl)amino]pentanoic acid (14). Deacetylcolchicine **13** (1.09 g, 3.00 mmol, 1.00 equiv.) was placed into a Schlenk flask, followed by the addition of dimethyl sulfoxide (10.9 mL), *N*-methylmorpholine (4.17 mL), and then glutaric anhydride (0.37 g, 3.51 mmol, 1.17 equiv.) under an inert atmosphere. The resulting mixture was stirred for 1 h at 50 °C, neutralized with a saturated solution of NH_4Cl, diluted with distilled water (50 mL), and extracted with ethyl acetate. The combined organic layer was dried with Na_2SO_4, the solvent was evaporated under reduced pressure. The product was purified by column chromatography (eluent $CHCl_3$—MeOH (10 : 1)) to afford product **14** (636 mg, 45%) as orange crystals. M.p. 129 °C. ^{1}H NMR, δ: 12.01 (br.s, 1 H, COOH(5a)); 8.53 (d, 1 H, NH, J = 8.2 Hz); 7.94 (d, 1 H, H(8), J = 1.6 Hz); 7.87 (dd, 1 H, H(11), J = 8.0 Hz, J = 1.8 Hz); 7.45 (d, 1 H, H(12), J = 8.0 Hz); 6.81 (s, 1 H, H(4)); 4.53 (dt, 1 H, H(7), J = 11.2 Hz, J = 7.5 Hz); 3.85 (s, 3 H, OCH_3); 3.83 (s, 3 H, OCH_3); 3.77 (s, 3 H, OCH_3); 3.49 (s, 3 H, OCH_3); 2.25—2.12 (m, 5 H, H(6), H(2a), H(4a)); 2.05—1.81 (m, 3 H, H(5), H(4a)); 1.76—1.63 (m, 2 H, H(3a)). ^{13}C NMR, δ: 177.90, 170.94, 163.43, 152.85, 150.69, 150.68, 150.37, 140.71, 135.13, 134.23, 134.12, 130.25, 125.40, 112.04, 107.71, 65.92, 60.75, 60.59, 55.96, 55.82, 54.91, 51.12, 34.22, 29.16, 26.27. Found (%): C, 63.72; H, 6.41. $C_{25}H_{29}NO_8$. Calculated (%): C, 63.68; H, 6.20.

(*S*)-6-Amino-*N*-(1,2,3,10-tetramethoxy-9-oxo-5,6,7,9-tetrahydrobenzo[*a*]heptalen-7-yl)hexanamide (15). Deacetylcolchicine **13** (771 mg, 2.16 mmol, 1.00 equiv.), 6-(*tert*-butoxycarbonylamino)hexanoic acid (549 mg, 2.38 mmol, 1.10 equiv.), and *N*-hydroxysuccinimide (189 mg, 1.64 mmol, 0.76 equiv.) were placed into a Schlenk flask and filled it with argon, followed by the addition of anhydrous $CHCl_3$ (20.0 mL), triethylamine (903 μL, 6.48 mmol, 3.00 equiv.), and diisopropylcarbodiimide (461 μL, 3.24 mmol, 1.50 equiv.). The mixture was stirred for 20 h at room temperature, diluted with distilled water (50 mL), and extracted with $CHCl_3$ (2×30 mL). The combined organic layer was dried with Na_2SO_4, the solvent was evaporated under reduced pressure. The residue was dissolved in dichloromethanee (30.0 mL), followed by the addition of trifluoroacetic acid (7.0 mL). The resulting mixture was stirred for 1.5 h at room temperature, neutralized with a saturated solution of Na_2CO_3, and extracted with dichloromethane (2×30 mL). The combined organic layer was dried with Na_2SO_4, the solvent was evaporated under reduced pressure. The product was purified by column chromatography (eluent $CHCl_3$—MeOH (12 : 1)) to afford product **15** (599 mg, 59%) as an orange foam. M.p. 117 °C. ^{1}H NMR, δ: 8.53 (d, 1 H, N(7)H, J = 8.2 Hz); 7.97 (s, 1 H, H(8)); 7.89 (d, 1 H, H(11), J = 8.0 Hz); 7.46 (d, 1 H, H(12), J = 8.0 Hz); 6.83 (s, 1 H, H(4)); 4.60—4.50 (m, 1 H, H(7));

3.87 (s, 3 H, OCH_3); 3.85 (s, 3 H, OCH_3); 3.79 (s, 3 H, OCH_3); 3.63 (dd, 2 H, H(2a), J = 13.7 Hz, J = 6.8 Hz); 3.52 (s, 3 H, OCH_3); 3.04 (dd, 4 H, H(3a), H(6a), J = 9.9 Hz, J = 5.8 Hz); 2.58—2.53 (m, 2 H, H(6)); 2.32—2.24 (m, 4 H, H(4a), H(5a)); 2.19—2.13 (br.s, 2 H, NH_2); 2.05—1.92 (m, 2 H, H(5)). ^{13}C NMR, δ: 176.89, 171.51, 166.31, 153.10, 150.35, 141.04, 140.54, 139.25, 134.94, 129.92, 128.02, 126.80, 124.04, 123.30, 60.84, 60.56, 55.86, 52.08, 48.09, 40.65, 38.14, 35.34, 25.91, 25.21, 23.29, 22.96. Found (%): C, 66.51; H, 7.19. $C_{26}H_{34}N_2O_6$. Calculated (%): C, 66.36; H, 7.28.

Synthesis of derivatives 16 and 17 (general procedure). Compound **14** (70 mg, 0.15 mmol, 1.00 equiv.), EDC · HCl (45 mg, 0.29 mmol, 2.00 equiv.), DMAP (45.0 mg, 0.37 mmol, 2.46 equiv.), and terpenoid **7** or **8** (0.15 mmol, 1.00 equiv.) were dissolved in anhydrous dichloromethane (12.0 mL) under an argon atmosphere. The mixture was stirred for 16 h at room temperature and the solvent was evaporated under reduced pressure. The residue was diluted with distilled water (15.0 mL) and extracted with EtOAc (20×3 mL). The combined organic layer was dried with Na_2SO_4, the solvent was evaporated under reduced pressure. The product was purified by column chromatography.

***N*^{1}-((*S*)-1,2,3,10-Tetramethoxy-9-oxo-5,6,7,9-tetrahydrobenzo[*a*]heptalen-7-yl)-*N*^{5}-((1*R*,2*R*,4*R*)-1,7,7-trimethylbicyclo[2.2.1]heptan-2-yl)glutaramide (16).** The eluent for column chromatography was petroleum ether—EtOAc—EtOH (6 : 1 : 1). The yield was 75 mg (83%), a beige powder. M.p. 122 °C. ^{1}H NMR, δ: 8.53 (d, 1 H, N(1a)H, J = 8.1 Hz); 7.96 (s, 1 H, H(8)); 7.88 (dd, 1 H, N(7a)H, J = 8.0 Hz, J = 1.6 Hz); 7.46 (d, 1 H, H(11), J = 8.0 Hz); 7.12 (d, 1 H, H(12), J = 7.9 Hz); 6.83 (s, 1 H, H(4)); 4.55 (dt, 1 H, H(7), J = 10.5 Hz, J = 7.4 Hz); 3.86 (s, 3 H, OCH_3); 3.85 (s, 3 H, OCH_3); 3.79 (s, 3 H, OCH_3); 3.71 (dd, 1 H, H(1′), J = 14.7 Hz, J = 8.0 Hz); 3.51 (s, 3 H, OCH_3); 2.58—2.52 (m, 1 H, H(5′)$_{endo}$); 2.18 (dd, 3 H, H(4′)$_{exo}$, H(5), J = 9.3 Hz, J = 5.4 Hz); 2.09 (dd, 2 H, H(6), J = 13.2 Hz, J = 6.5 Hz); 2.02 (dd, 1 H, H(4′)$_{endo}$, J = 13.2 Hz, J = 7.0 Hz); 1.93 (dd, 1 H, H(3′), J = 15.4 Hz, J = 8.1 Hz); 1.77—1.67 (m, 2 H, H(5a)); 1.66—1.53 (m, 4 H, H(3a), H(4a)); 1.47 (t, 1 H, H(2′)$_{endo}$, J = 9.6 Hz); 1.08 (dt, 2 H, H(5′)$_{endo}$, H(2′)$_{exo}$, J = 14.0 Hz, J = 7.5 Hz); 0.86 (s, 3 H, C(10′)H_3); 0.75 (s, 3 H, C(9′)H_3); 0.73 (s, 3 H, C(8′)H_3). ^{13}C NMR, δ: 171.53, 171.22, 166.31, 153.09, 150.36, 141.01, 140.54, 139.24, 134.96, 129.92, 128.06, 126.80, 124.05, 123.31, 108.24, 60.84, 60.58, 55.88, 55.86, 52.05, 48.63, 48.14, 46.37, 44.23, 38.10, 37.03, 35.72, 34.76, 29.85, 26.75, 21.90, 20.39, 19.93, 19.75, 18.46. Found (%): C, 69.47; H, 7.52. $C_{35}H_{46}N_2O_7$. Calculated (%): C, 69.28; H, 7.64.

5-Oxo-*N*-((*S*)-1,2,3,10-tetramethoxy-9-oxo-5,6,7,9-tetrahydrobenzo[*a*]heptalen-7-yl)-5-[2-((1*R*,4*S*)-1,3,3-trimethylbicyclo[2.2.1]heptan-2-ylidene)hydrazinyl]pentanamide (17). The eluent for column chromatography was petroleum ether—EtOAc—EtOH (7 : 1 : 1). The yield was 64 mg (69%), a white powder. M.p. 136 °C. ^{1}H NMR, δ: 9.09 (d, 1 H, N(7a)H, J = 7.7 Hz); 8.55 (dd, 1 H, N(1a)H, J = 16.3 Hz, J = 7.9 Hz); 7.96 (s, 1 H, H(8)); 7.88 (d, 1 H, H(11), J = 8.0 Hz); 7.46 (d, 1 H, H(12), J = 8.0 Hz); 6.82 (s, 1 H, H(4)); 4.61—4.50 (m, 1 H, H(7)); 3.85 (s, 3 H, OCH_3); 3.85 (s, 3 H, OCH_3); 3.79 (s, 3 H, OCH_3); 3.50 (s, 3 H, OCH_3); 2.58—2.52 (m, 1 H, H(5′)$_{exo}$); 2.27—2.14 (m, 4 H, H(5), H(6)); 2.04—1.91 (m, 2 H, H(4′)$_{exo}$, H(4′)$_{endo}$); 1.81 (s, 1 H, H(3′)); 1.78—1.70 (m, 2 H, H(5a)); 1.69—1.59 (m, 2 H, H(4a)); 1.52 (d, 2 H, H(3a), J = 6.6 Hz); 1.33 (d, 1 H, H(5′)$_{endo}$, J = 9.8 Hz); 1.24 (s, 3 H, C(10′)H_3); 1.20 (s, 1 H, H(7′)); 1.17 (s, 3 H, C(8′)H_3); 1.14 (s, 1 H, H(7′)); 1.06 (s, 3 H, C(9′)H_3). ^{13}C NMR, δ: 174.05, 171.23, 166.47, 166.28, 153.10, 150.38, 140.96, 140.56, 139.24, 134.94, 129.92, 128.07, 126.82, 124.04, 123.32, 108.25, 60.83, 60.81, 60.58, 60.58, 55.87, 52.03, 50.93, 49.33, 48.11, 42.28, 41.90, 38.22, 33.90, 29.86, 24.65, 22.33, 21.49, 20.60, 17.16. Found (%): C, 67.59; H, 7.51. $C_{35}H_{45}N_3O_7$. Calculated (%): C, 67.83; H, 7.32.

Synthesis of derivatives 18 and 19 (general procedure). Compound **14** (100 mg, 0,21 mmol, 1.00 equiv.) was placed into a Schlenk flask and filled it with argon, followed by the addition of CH_2Cl_2 (10.0 mL), Et_3N (134 μL, 0.96 mmol, 4.6 equiv.), and 2,4,6-trichlorobenzoyl chloride (TCBC, Yamaguchi′s reagent) (59 μL, 0.38 mmol, 1.80 equiv.) at 0 °C. The mixture was stirred for 5 h with an increase in temperature from 0 °C to 20 °C, then a solution of DMAP (77 mg, 0.63 mmol, 3.00 equiv.) and terpenoid **5** or **6** (0.21 mmol, 1.00 equiv.) in CH_2Cl_2 (6.00 mL) was added dropwise. The resulting mixture was stirred for 20 h at room temperature, the solvent was evaporated under reduced pressure, the product was purified by column chromatography.

(1*S*,2*R*,4*S*)-1,7,7-Trimethylbicyclo[2.2.1]heptan-2-yl-5-oxo-5-[((*S*)-1,2,3,10-tetramethoxy-9-oxo-5,6,7,9-tetrahydrobenzo[*a*]heptalen-7-yl)amino]pentanoate (18). The eluent for column chromatography was petroleum ether—EtOAc—EtOH (7 : 1 : 1). The yield was 89 mg (70%), a beige powder. M.p. 124 °C. ^{1}H NMR, δ: 8.54 (d, 1 H, N(1a)H, J = 8.1 Hz); 7.94 (s, 1 H, H(8)); 7.87 (d, 1 H, H(11), J = 8.0 Hz); 7.44 (d, 1 H, H(12), J = 8.0 Hz); 6.81 (s, 1 H, H(4)); 4.78 (d, 1 H, H(1′), J = 9.6 Hz); 4.59—4.48 (m, 1 H, H(7)); 3.84 (s, 3 H, OCH_3); 3.83 (s, 3 H, OCH_3); 3.77 (s, 3 H, OCH_3); 3.49 (s, 3 H, OCH_3); 2.56—2.51 (m, 1 H, H(5′)$_{exo}$); 2.32—2.26 (m, 2 H, H(5)); 2.25—2.13 (m, 4 H, H(6), H(4′)$_{endo}$, H(4′)$_{exo}$); 2.03—1.88 (m, 2 H, H(5a)); 1.87—1.79 (m, 1 H, H(3′)); 1.76—1.69 (m, 2 H, H(3a)); 1.69—1.60 (m, 2 H, H(4a)); 1.23—1.12 (m, 2 H, H(2′)$_{exo}$, H(2′)$_{endo}$); 0.90 (d, 1 H, H(5′)$_{endo}$, J = 3.7 Hz); 0.84 (s, 3 H, C(8′)H_3); 0.82 (s, 3 H, C(9′)H_3); 0.74 (s, 3 H, C(10′)H_3). ^{13}C NMR, δ: 172.68, 170.89, 166.26, 153.10, 150.36, 140.93, 140.54, 139.24, 134.93, 129.94, 128.05, 126.82, 123.98, 123.27, 108.24, 78.62, 60.84, 60.56, 55.86, 52.04, 48.37, 48.16, 47.39, 44.21, 38.12, 36.25, 34.30, 33.22, 29.84, 27.57, 26.67, 20.76,

19.50, 18.58, 13.39. Found (%): C, 69.35; H, 7.19. $C_{35}H_{45}NO_8$. Calculated (%): C, 69.17; H, 7.46.

2-{[(1*R*,4*R*,*E*)-1,7,7-Trimethylbicyclo[2.2.1]heptan-2-ylidene]amino}ethyl 5-oxo-5-{[(*S*)-1,2,3,10-tetramethoxy-9-oxo-5,6,7,9-tetrahydrobenzo[*a*]heptalen-7-yl]amino}pentanoate (19). The eluent for column chromatography was petroleum ether—EtOAc—EtOH (7 : 1 : 1). The yield was 107 mg (79%), a light brown powder. M.p. 137 °C. ^{1}H NMR, δ: 8.54 (d, 1 H, N(1a)H, *J* = 8.1 Hz); 7.95 (d, 1 H, H(8); *J* = 1.6 Hz); 7.88 (dd, 1 H, H(11), *J* = 8.0 Hz, *J* = 1.7 Hz); 7.46 (d, 1 H, H(12), *J* = 8.0 Hz); 6.82 (s, 1 H, H(4)); 4.54 (dt, 1 H, H(7), *J* = 11.3 Hz, *J* = 7.5 Hz); 4.16 (td, 2 H, H(7a), *J* = 6.0 Hz, *J* = 1.3 Hz); 3.86 (s, 3 H, OCH_3); 3.85 (s, 3 H, OCH_3); 3.79 (s, 3 H, OCH_3); 3.50 (s, 3 H, OCH_3); 3.39—3.35 ((m, 1 H, H(2′)$_{endo}$); 2.58—2.52 (m, 1 H, H(5′)$_{exo}$); 2.29—2.15 (m, 6 H, H(5a), H(5), H(6)); 2.06—1.98 (m, 1 H, H(4′)$_{endo}$); 1.97—1.89 (m, 1 H, H(4′)$_{exo}$); 1.86—1.77 (m, 2 H, H(4a)); 1.76—1.67 (m, 3 H, H(3a); H(3′)); 1.60—1.53 (m, 1 H, H(2′)$_{exo}$); 1.25—1.17 (m, 1 H, H(5′)$_{endo}$); 1.17—1.06 (m, 2 H, H(8a)); 0.84 (s, 3 H, C(8′)H$_3$); 0.82 (s, 3 H, C(9′)H$_3$); 0.64 (s, 3 H, C(10′)H$_3$). ^{13}C NMR, δ: 182.25, 172.49, 170.84, 166.26, 153.09, 150.37, 140.91, 140.55, 139.23, 134.91, 129.93, 128.05, 126.82, 123.97, 123.30, 108.23, 64.03, 60.82, 60.57, 55.85, 53.28, 52.04, 50.14, 48.17, 46.38, 43.17, 38.12, 35.01, 34.22, 32.80, 31.80, 29.83, 26.91, 20.67, 19.17, 18.69, 11.46. Found (%): C, 68.37; H, 7.60. $C_{37}H_{48}N_2O_8$. Calculated (%): C, 68.50; H, 7.46.

6-{[((1*S*,4*R*)-7,7-Dimethyl-2-oxobicyclo[2.2.1]heptan-1-yl)methyl]sulfonamido}-*N*-((*S*)-1,2,3,10-tetramethoxy-9-oxo-5,6,7,9-tetrahydrobenzo[*a*]heptalen-7-yl)hexanamide (20). Compound **15** (150 mg, 0,32 mmol, 2.00 equiv.) and DMAP (4 mg, 0.03 mmol, 0.10 equiv.) were placed into a Schlenk flask and filled it with argon, followed by the addition of acetonitrile (4.00 mL). Then a solution of camphorsulfonyl chloride **9** (40 mg, 0.16 mmol, 1.00 equiv.) in MeCN (3.00 mL) was added dropwise to the resulting solution at 0 °C over 1 h. The mixture was stirred for 20 h at room temperature, the solvent was evaporated under reduced pressure. The product was purified by column chromatography (eluent petroleum ether—ethyl acetate—ethanol (4 : 1 : 1)). The yield was 26 mg (24%), a light brown powder. M.p. 133 °C. ^{1}H NMR, δ: 8.52 (d, 1 H, N(1a)H, *J* = 8.1 Hz); 7.97 (d, 1 H, H(8), *J* = 1.6 Hz); 7.88 (dd, 1 H, H(11), *J* = 8.0 Hz, *J* = 1.7 Hz); 7.46 (d, 1 H, H(12), *J* = 8.0 Hz); 6.96 (t, 1 H, H(8a), *J* = 5.9 Hz); 6.82 (s, 1 H, H(4)); 4.60—4.50 (m, 1 H, H(7)); 3.87 (s, 3 H, OCH_3); 3.85 (s, 3 H, OCH_3); 3.79 (s, 3 H, OCH_3); 3.51 (s, 3 H, OCH_3); 3.04 (dd, 2 H, H(9a), *J* = 10.0 Hz, *J* = 5.9 Hz); 2.95 (dt, 2 H, H(7a), *J* = 12.8 Hz, *J* = 6.8 Hz); 2.58—2.52 (m, 1 H, H(5′)$_{exo}$); 2.30—2.25 (m, 4 H, H(5), H(6)); 2.21—2.15 (m, 2 H, H(4′)); 1.68—1.62 (m, 4 H, H(3′), H(2′)$_{endo}$, H(3a)); 1.53—1.47 (m, 6 H, H(4a), H(5), H(6a)); 1.38—1.34 (m, 1 H, H(2′)$_{exo}$); 1.30—1.28 (m, 1 H, H(5′)$_{endo}$); 1.01 (s, 3 H, C(8′)H$_3$); 0.79 (s, 3 H, C(9′)H$_3$). ^{13}C NMR, δ: 176.90, 171.47, 166.30, 153.09, 150.36, 141.02, 140.54, 139.25, 134.94, 129.93, 128.03, 126.81, 123.30, 108.24, 60.84, 60.57, 57.82, 55.86, 52.08, 47.56, 47.40, 42.51, 42.05, 41.99, 41.43, 38.15, 36.41, 29.98, 29.80, 29.47, 26.26, 25.79, 24.46, 22.96, 19.45, 19.29. Found (%): C, 63.45; H, 7.23. $C_{36}H_{48}N_2O_9S$. Calculated (%): C, 63.14; H, 7.06.

(1*S*,2*R*,4*S*)-1,7,7-Trimethylbicyclo[2.2.1]heptan-2-yl-{6-oxo-6-[((*S*)-1,2,3,10-tetramethoxy-9-oxo-5,6,7,9-tetrahydrobenzo[*a*]heptalen-7-yl)amino]hexyl}glycinate (21). Compound **15** (100 mg, 0.21 mmol, 1.00 equiv.) was placed into a Schlenk flask and filled it with argon, followed by the addition of dichloromethane (10.0 mL), Et_3N (88 μL, 0.63 mmol, 3.00 equiv.) and a dropwise addition of a solution of borneol chloroacetate **10** (91 mg, 0,42 mmol, 2.00 equiv.) in CH_2Cl_2 (5.00 mL). The mixture was stirred for 16 h at room temperature, the solvent was evaporated under reduced pressure. The product was purified by column chromatography (eluent petroleum ether—ethyl acetate—ethanol (5 : 1 : 1)). The yield was 27 mg (20%), an oily liquid. ^{1}H NMR, δ: 8.49 (d, 1 H, N(1a)H, *J* = 7.6 Hz); 7.14—7.06 (m, 2 H, H(8), H(12)); 7.01 (d, 1 H, H(11), *J* = 11.0 Hz); 6.76 (s, 1 H, H(4)); 4.85—4.82 (m, 1 H, N(8a)H); 4.81 (d, 1 H, H(1′), *J* = 2.9 Hz); 4.36—4.27 (m, 1 H, H(7)); 3.86 (s, 3 H, OCH_3); 3.83 (s, 3 H, OCH_3); 3.78 (s, 3 H, OCH_3); 3.52 (s, 3 H, OCH_3); 3.48 (br.s, 2 H, H(9a)); 2.60—2.56 (m, 2 H, H(7a)); 2.31—2.19 (m, 3 H, H(5), H(5′)$_{exo}$); 2.10 (t, 2 H, H(6), *J* = 7.0 Hz); 2.03—1.95 (m, 1 H, H(3′)); 1.89—1.80 (m, 3 H, H(4′), H(2′)$_{endo}$); 1.65—1.62 (m, 2 H, H(3a)); 1.45—1.35 (m, 4 H, H(5a), H(6a)); 1.21—1.11 (m, 4 H, H(5′)$_{endo}$, H(2′)$_{exo}$, H(4a)); 0.86 (s, 3 H, C(8′)H$_3$); 0.83 (s, 3 H, C(9′)H$_3$); 0.76 (s, 3 H, C(10′)H$_3$). ^{13}C NMR, δ: 177.92, 171.38, 170.96, 163.49, 152.89, 150.76, 150.44, 140.72, 135.16, 134.30, 134.19, 130.38, 125.46, 112.04, 107.68, 78.99, 60.82, 60.66, 55.99, 55.82, 54.80, 53.42, 51.12, 48.37, 47.38, 44.18, 36.22, 35.72, 35.10, 29.23, 27.55, 27.03, 26.75, 26.17, 25.04, 19.49, 18.56, 13.38. Found (%): C, 68.54; H, 7.68. $C_{38}H_{52}N_2O_8$. Calculated (%): C, 68.65; H, 7.88.

Molecular docking. Molecular docking was carried out in the Schrodinger Maestro environment using applications from the Schrodinger Small Molecule Drug Discovery Suite 2017-1.[53] Three-dimensional structures of compounds were obtained empirically in the LigPrep application using the OPLS3 force field.[54] All possible tautomeric forms of compounds were taken into account, as well as all ionized forms of compounds in the pH range of 7.0±2.0. The X-ray diffraction model of the main protease of SARS-CoV-2 virus co-crystallized with the non-covalent inhibitor ML188 (PDB ID 7L0D,[54] resolution 2.39 Å) was used for calculations. To model the possible mechanism of binding to the selected target, molecular docking of compounds in the ML188 binding site of the main protease of SARS-CoV-2 in the Glide application was performed.[55] The search area for the calculated docking function was automatically selected based on the size

and physicochemical properties of ML188. The algorithm of increased docking accuracy XP (*extra precision*) was used. The IFD (Induced Fit Docking) molecular modeling protocol was used, which takes into account the flexibility of the side chains of amino acid residues of the active site of the target during docking.[56] Docking was performed in comparison with the IFD results obtained for the best conformation of the inhibitor ML188 closest to the X-ray diffraction data. The free energy (d*G*) of non-covalent complexes formed during the IFD protocol was calculated by the MM/GBSA method[57] using Prime.[58] Non-covalent interactions of compounds at the binding site were visualized using the Biovia Discovery Studio Visualizer.[59]

Free energy calculations by the SQM method were performed in the MOPAC 2016 program[60] using the PM6-D3H4/COSMO system.[61,62] The dielectric constant (EPS) was set at 78.4. The operators MOZYME and LARGE were used. To improve the accuracy of the COSMO model calculations, the number of geometric segments per atom (NSPA) was set to 92. To avoid local energy minima associated with protein conformations, as well as to reduce computational costs, we performed SQM optimization for the ligand—protein system within the active site of the main protease at a distance of up to 8 Å from the ligand. This distance was chosen on the basis of minor differences in the coordinates of the atoms of amino acid residues located farther in all complexes obtained as a result of the IFD protocol.

Molecular dynamics modeling was performed using NAMD 2.13.[63] The ligand—protein complexes with the lowest estimated binding energies from IFD results were selected to initiate molecular dynamics. Ligand parameters were analyzed on the SwissParam online server[64] using the CHARMM force field22.[65] Complex preparation, solvation, and neutralization were performed in the VMD program.[66] Ligand—protein complexes were placed in a water cube (solvent model TIP3P) with a minimum buffer zone of 5 Å from protein surface. The system was neutralized by adding sodium and chlorine ions to obtain a 0.15 *M* aqueous solution of sodium chloride. Energy minimization was carried out over 2000 iterations using the steepest descent method.[67] The complexes were heated to 310 K and equilibrated in the NVT ensemble for 1 ns at 310 K. Molecular dynamics simulations were performed for 100 ns in the NVT ensemble under periodic boundary conditions. The trajectory of each complex was analyzed using the VEGA ZZ software package.[68]

Biological studies. ***MTT analysis.*** Cytotoxic activity of colchicine **1** and compounds **16—21** was evaluated using a standard test with 3-(4,5-dimethyl-2-thiazolyl)-2,5-diphenyl-2*H*-tetrazolium bromide (MTT, Sigma). The stock solution of test compounds in DMSO with a concentration of 20 mmol L^{-1} was stored at −20 °C until use. Solutions of the test compounds (100 μL) in various concentrations were placed in the wells, the range of dilutions ranged from 20 μmol L^{-1} to 0.001 nmol L^{-1}. Cells were added in an amount of $5—10 \cdot 10^3$ per well. Untreated cells served as a control group. Cells were incubated for 72 h. In the last 4 h, 10 μL of a MTT solution with a concentration of 5 mg mL^{-1} was added in each well. After incubation, the growth medium was removed and 100 μL of DMSO was added to each well. The plates were incubated on a shaker for 15 min to dissolve the formed formazan. The optical density was determined on a Titertek spectrophotometer (UK) at 540 nm. The results were analyzed using the Excel program (Microsoft). The cytotoxic concentration leading in 50% of the maximum toxic effect (IC_{50}) was calculated from the titration curves. Proliferation inhibition (inhibition index, II) was calculated as

$$II = [1 - (D_{exp}/D_{control})],$$

where D_{exp} and $D_{control}$ are the optical densities in experimental and control samples, respectively.

Inhibitory activity against viral protease. The activity of the 3CL viral protease was measured using a fluorogenic substrate DabcylKTSAVLQ↓SGFRKME(Edans) NH2 on a CLARIOstar Plus instrument (BMG Labtech, Germany) at wavelengths of 355 and 460 nm for excitation/emission, respectively. Reaction mixtures were prepared in 384-well plate, incubated for 30 min, and measurements were carried out at 30 °C. Each well contained one reaction mixture: buffer TrisHCl (pH 7.3, 20 m*M* of Tris, 100 m*M* of NaCl, 1 m*M* of EDTA, 1 m*M* of DTT), 10 μ*M* of substrate, 400 μ*M* of inhibitor, and 300 n*M* of Mpro. The instrument was calibrated according to a solution of the peptide subjected to complete hydrolysis. The fluorescence value of this mixture was taken as 80%. The measurement was carried out in the kinetic scanning mode (50 cycles of 10 s). All experiments were performed in triplicate ($n = 3$). The preinstalled MARS Data Analysis software (BMG LABTECH, Germany) was used for calculations. The IC_{50} value was taken as the concentration of the test compound at which the fluorescence level decreased by 50% of the maximum observed without the addition of the inhibitor.

Synthesis of all compounds and biological studies were financially supported by the Russian Science Foundation (Project No. 19-13-00158). Molecular docking was carried out with the financial support from the Ministry of Science and Higher Education of the Russian Federation (Agreement No. 075-15-2021-1355 of October 12, 2021) in the framework of the implementation of selected activities of the Federal Scientific and Technical Program for the Development of Synchrotron and Neutron Research and Research Infrastructure for 2019—2027 years.

No human or animal subjects were used in this research.

The authors declare no competing interests.

References

1. J. H. Beigel, K. M. Tomashek, L. E. Dodd, A. K. Mehta, B. S. Zingman, A. C. Kalil, E. Hohmann, H. Y. Chu, A. Luetkemeyer, S. Kline, D. Lopez de Castilla, R. W. Finberg, K. Dierberg, V. Tapson, L. Hsieh, T. F. Patterson, R. Paredes, D. A. Sweeney, W. R. Short, G. Touloumi, D. C. Lye, N. Ohmagari, M. Oh, G. M. Ruiz-Palacios, T. Benfield, G. Fätkenheuer, M. G. Kortepeter, R. L. Atmar, C. B. Creech, J. Lundgren, A. G. Babiker, S. Pett, J. D. Neaton, T. H. Burgess, T. Bonnett, M. Green, M. Makowski, A. Osinusi, S. Nayak, H. C. Lane, *New Engl. J. Med.*, 2020, **383**, 1813—1826; DOI: 10.1056/NEJMoa2007764.
2. A. Jayk Bernal, M. M. Gomes da Silva, D. B. Musungaie, E. Kovalchuk, A. Gonzalez, V. Delos Reyes, A. Martín-Quirós, Y. Caraco, A. Williams-Diaz, M. L. Brown, J. Du, A. Pedley, C. Assaid, J. Strizki, J. A. Grobler, H. H. Shamsuddin, R. Tipping, H. Wan, A. Paschke, J. R. Butterton, M. G. Johnson, C. De Anda, *New Engl. J. Med.*, 2022, **386**, 509—520; DOI: 10.1056/NEJMoa2116044.
3. R. Abdelnabi, C. S. Foo, D. Jochmans, L. Vangeel, S. De Jonghe, P. Augustijns, R. Mols, B. Weynand, T. Wattanakul, R. M. Hoglund, J. Tarning, C. E. Mowbray, P. Sjö, F. Escudié, I. Scandale, E. Chatelain, J. Neyts, *Nat. Commun.*, 2022, **13**, 719; DOI: 10.1038/s41467-022-28354-0.
4. H. M. Dabbous, S. Abd-Elsalam, M. H. El-Sayed, A. F. Sherief, F. F. S. Ebeid, M. S. A. El Ghafar, S. Soliman, M. Elbahnasawy, R. Badawi, M. A. Tageldin, *Arch. Virol.*, 2021, **166**, 949—954; DOI: 10.1007/s00705-021-04956-9.
5. K. Srinivasan, M. Rao, *Ther. Adv. Infect. Dis.*, 2021, **8**; DOI: 10.1177/20499361211063016.
6. J. Y. Kim, Y. R. Jang, J. H. Hong, J. G. Jung, J.-H. Park, A. Streinu-Cercel, A. Streinu-Cercel, O. Săndulescu, S. J. Lee, S. H. Kim, N. H. Jung, S. G. Lee, J. E. Park, M. K. Kim, D. B. Jeon, Y. J. Lee, B. S. Kim, Y. M. Lee, Y.-S. Kim, *Clin. Ther.*, 2021, **43**, 1706—1727; DOI: 10.1016/j.clinthera.2021.08.009.
7. T. Kim, D.-H. Joo, S. W. Lee, J. Lee, S. J. Lee, J. Kang, *J. Clin. Med.*, 2022, **11**, 1412; DOI: 10.3390/jcm11051412.
8. E. Miguez-Rey, D. Choi, S. Kim, S. Yoon, O. Săndulescu, *Expert Opin. Invest. Drugs*, 2022, **31**, 41—58; DOI: 10.1080/13543784.2022.2030310.
9. Y. Y. Syed, *Drugs*, 2020, **80**, 91—97; DOI: 10.1007/s40265-019-01252-4.
10. M. Scarsi, S. Piantoni, E. Colombo, P. Airó, D. Richini, M. Miclini, V. Bertasi, M. Bianchi, D. Bottone, P. Civelli, M.-S. Cotelli, E. Damiolini, G. Galbassini, D. Gatta, M.-L. Ghirardelli, R. Magri, P. Malamani, M. Mendeni, S. Molinari, A. Morotti, L. Salada, M. Turla, A. Vender, A. Tincani, A. Brucato, F. Franceschini, R. Furloni, L. Andreoli, *Ann. Rheum. Dis.*, 2020, **79**, 1286—1289; DOI: 10.1136/annrheumdis-2020-217712.
11. S. G. Deftereos, G. Siasos, G. Giannopoulos, D. A. Vrachatis, C. Angelidis, S. G. Giotaki, P. Gargalianos, H. Giamarellou, C. Gogos, G. Daikos, M. Lazanas, P. Lagiou, G. Saroglou, N. Sipsas, S. Tsiodras, D. Chatzigeorgiou, N. Moussas, A. Kotanidou, N. Koulouris, E. Oikonomou, A. Kaoukis, C. Kossyvakis, K. Raisakis, K. Fountoulaki, M. Comis, D. Tsiachris, E. Sarri, A. Theodorakis, L. Martinez-Dolz, J. Sanz-Sánchez, B. Reimers, G. G. Stefanini, M. Cleman, D. Filippou, C. D. Olympios, V. N. Pyrgakis, J. Goudevenos, G. Hahalis, T. M. Kolettis, E. Iliodromitis, D. Tousoulis, C. Stefanadis, *Hell. J. Cardiol.*, 2020, **61**, 42—45; DOI: 10.1016/j.hjc.2020.03.002.
12. N. Schlesinger, B. L. Firestein, L. Brunetti, *Curr. Pharmacol. Rep.*, 2020, **6**, 137—145; DOI: 10.1007/s40495-020-00225-6.
13. M. I. Lopes, L. P. Bonjorno, M. C. Giannini, N. B. Amaral, P. I. Menezes, S. M. Dib, S. L. Gigante, M. N. Benatti, U. C. Rezek, L. L. Emrich-Filho, B. A. A. Sousa, S. C. L. Almeida, R. Luppino Assad, F. P. Veras, A. Schneider, T. S. Rodrigues, L. O. S. Leiria, L. D. Cunha, J. C. Alves-Filho, T. M. Cunha, E. Arruda, C. H. Miranda, A. Pazin-Filho, M. Auxiliadora-Martins, M. C. Borges, B. A. L. Fonseca, V. R. Bollela, C. M. Del-Ben, F. Q. Cunha, D. S. Zamboni, R. C. Santana, F. C. Vilar, P. Louzada-Junior, R. D. R. Oliveira, *RMD Open*, 2021, **7**, e001455; DOI: 10.1136/rmdopen-2020-001455.
14. V. Yu. Mareev, Ya. A. Orlova, A. G. Plisyuk, E. P. Pavlikova, Zh. A. Akopyan, S. T. Matskeplishvili, P. S. Malakhov, T. N. Krasnova, E. M. Seredenina, A. V. Potapenko, M. A. Agapov, D. A. Asratyan, L. I. Dyachuk, L. M. Samohodskaya, E. A. Mershina, V. E. Sinitsin, P. V. Pakhomov, E. A. Zhdanova, Yu. V. Mareev, Yu. L. Begrambekova, A. A. Kamalov, *Kardiologiya* [*Cardiology*], 2021, **61**, 15—27; DOI: 10.18087/cardio.2021.2.n1560 (in Russian).
15. A. Bonaventura, A. Vecchié, L. Dagna, F. Tangianu, A. Abbate, F. Dentali, *Inflamm. Res.*, 2022, **71**, 293—307; DOI: 10.1007/s00011-022-01540-y.
16. I. A. Gracheva, E. S. Shchegravina, H. G. Schmalz, I. P. Beletskaya, A. Y. Fedorov, *J. Med. Chem.*, 2020, **63**, 10618—10651; DOI: 10.1021/acs.jmedchem.0c00222.
17. E. S. Shchegravina, E. V. Svirshchevskaya, S. Combes, D. Allegro, P. Barbier, B. Gigant, P. F. Varela, A. E. Gavryushin, D. A. Kobanova, A. E. Shchekotikhin, A. Yu. Fedorov, *Eur. J. Med. Chem.*, 2020, **207**, 112724; DOI: 10.1016/j.ejmech.2020.112724.
18. E. S. Shchegravina, A. A. Maleev, S. K. Ignatov, I. A. Gracheva, A. Stein, H.-G. Schmalz, A. E. Gavryushin, A. Zubareva, E. V. Svirshchevskaya, A. Yu. Fedorov, *Eur. J. Med. Chem.*, 2017, **141**, 51—60; DOI: 10.1016/j.ejmech.2017.09.055.

19. I. Gracheva, E. Svirshchevskaya, E. Zaburdaeva, A. Fedorov, *Synthesis*, 2017, **49**, 4335—4340; DOI: 10.1055/s-0036-1589060.
20. N. S. Sitnikov, A. S. Kokisheva, G. K. Fukin, J.-M. Neudörfl, H. Sutorius, A. Prokop, V. V. Fokin, H.-G. Schmalz, A. Yu. Fedorov, *Eur. J. Org. Chem.*, 2014, 6481—6492; DOI: 10.1002/ejoc.201402850.
21. S. Toldo, A. Abbate, *Nat. Rev. Cardiol.*, 2018, **15**, 203—214; DOI: 10.1038/nrcardio.2017.161.
22. Y. Y. Leung, L. L. Yao Hui, V. B. Kraus, *Semin. Arthritis Rheum.*, 2015, **45**, 341—350; DOI: 10.1016/j.semarthrit.2015.06.013.
23. M. Z. Tay, C. M. Poh, L. Rénia, P. A. MacAry, L. F. P. Ng, *Nat. Rev. Immunol.*, 2020, **20**, 363—374; DOI: 10.1038/s41577-020-0311-8.
24. M. Richter, V. Boldescu, D. Graf, F. Streicher, A. Dimoglo, R. Bartenschlager, C. D. Klein, *ChemMedChem*, 2019, **14**, 469—483; DOI: 10.1002/cmdc.201800641.
25. R. Paduch, M. Trytek, S. K. Król, J. Kud, M. Frant, M. Kandefer-Szerszeń, J. Fiedurek, *Pharm. Biol.*, 2016, **54**, 1096—1107; DOI: 10.3109/13880209.2015.1103753.
26. G. Wang, W. Tang, R. R. Bidigare, in *Natural Products*, Humana Press, Totowa, 2005, pp. 197—227.
27. C.-C. Wen, Y.-H. Kuo, J.-T. Jan, P.-H. Liang, S.-Y. Wang, H.-G. Liu, C.-K. Lee, S.-T. Chang, C.-J. Kuo, S.-S. Lee, C.-C. Hou, P.-W. Hsiao, S.-C. Chien, L.-F. Shyur, N.-S. Yang, *J. Med. Chem.*, 2007, **50**, 4087—4095; DOI: 10.1021/jm070295s.
28. T. H. J. Niedermeyer, U. Lindequist, R. Mentel, D. Gördes, E. Schmidt, K. Thurow, M. Lalk, *J. Nat. Prod.*, 2005, **68**, 1728—1731; DOI: 10.1021/np0501886.
29. O. I. Yarovaya, N. F. Salakhutdinov, *Russ. Chem. Rev.*, 2021, **90**, 488—510; DOI: 10.1070/rcr4969.
30. A. S. Sokolova, V. P. Putilova, O. I. Yarovaya, A. V. Zybkina, E. D. Mordvinova, A. V. Zaykovskaya, D. N. Shcherbakov, I. R. Orshanskaya, E. O. Sinegubova, I. L. Esaulkova, S. S. Borisevich, N. I. Bormotov, L. N. Shishkina, V. V. Zarubaev, O. V. Pyankov, R. A. Maksyutov, N. F. Salakhutdinov, *Molecules*, 2021, **26**, 2235; DOI: 10.3390/molecules26082235.
31. A. A. Kononova, A. S. Sokolova, S. V. Cheresiz, O. I. Yarovaya, R. A. Nikitina, A. A. Chepurnov, A. G. Pokrovsky, N. F. Salakhutdinov, *MedChemComm*, 2017, **8**, 2233—2237; DOI: 10.1039/C7MD00424A.
32. A. S. Sokolova, O. I. Yarovaya, A. V. Zybkina, E. D. Mordvinova, N. S. Shcherbakova, A. V. Zaykovskaya, D. S. Baev, T. G. Tolstikova, D. N. Shcherbakov, O. V. Pyankov, R. A. Maksyutov, N. F. Salakhutdinov, *Eur. J. Med. Chem.*, 2020, **207**, 112726; DOI: 10.1016/j.ejmech.2020.112726.
33. A. S. Sokolova, O. I. Yarovaya, M. D. Semenova, A. A. Shtro, I. R. Orshanskaya, V. V. Zarubaev, N. F. Salakhutdinov, *MedChemComm*, 2017, **8**, 960—963; DOI: 10.1039/C6MD00657D.
34. V. V. Zarubaev, A. V. Garshinina, T. S. Tretiak, V. A. Fedorova, A. A. Shtro, A. S. Sokolova, O. I. Yarovaya, N. F. Salakhutdinov, *Antiviral Res.*, 2015, **120**, 126—133; DOI: 10.1016/j.antiviral.2015.06.004.
35. Z. T. Muhseen, A. R. Hameed, H. M. H. Al-Hasani, M. Tahir ul Qamar, G. Li, *J. Mol. Liq.*, 2020, **320**, 114493; DOI: 10.1016/j.molliq.2020.114493.
36. S. V. Giofrè, E. Napoli, N. Iraci, A. Speciale, F. Cimino, C. Muscarà, M. S. Molonia, G. Ruberto, A. Saija, *Comput. Biol. Med.*, 2021, **134**, 104538; DOI: 10.1016/j.compbiomed.2021.104538.
37. B. Hou, Y.-M. Zhang, H.-Y. Liao, L.-F. Fu, D.-D. Li, X. Zhao, J.-X. Qi, W. Yang, G.-F. Xiao, L. Yang, Z.-Y. Zuo, L. Wang, X.-L. Zhang, F. Bai, L. Yang, G. F. Gao, H. Song, J.-M. Hu, W.-J. Shang, J. Zhou, *J. Nat. Prod.*, 2022, **85**, 327—336; DOI: 10.1021/acs.jnatprod.1c00805.
38. M. Z. Hassan, H. Osman, M. A. Ali, M. J. Ahsan, *Eur. J. Med. Chem.*, 2016, **123**, 236—255; DOI: 10.1016/j.ejmech.2016.07.056.
39. O. I. Artyushin, A. A. Moiseeva, V. V. Zarubaev, A. V. Slita, A. V. Galochkina, A. A. Muryleva, S. S. Borisevich, O. I. Yarovaya, N. F. Salakhutdinov, V. K. Brel, *Chem. Biodiversity*, 2019, **16**, e1900340; DOI: 10.1002/cbdv.201900340.
40. O. I. Yarovaya, K. S. Kovaleva, A. A. Zaykovskaya, L. N. Yashina, N. S. Scherbakova, D. N. Scherbakov, S. S. Borisevich, F. I. Zubkov, A. S. Antonova, R. Y. Peshkov, I. V. Eltsov, O. V. Pyankov, R. A. Maksyutov, N. F. Salakhutdinov, *Bioorg. Med. Chem. Lett.*, 2021, **40**, 127926; DOI: 10.1016/j.bmcl.2021.127926.
41. A. S. Sokolova, O. I. Yarovaya, A. V. Shernyukov, Y. V. Gatilov, Y. V. Razumova, V. V. Zarubaev, T. S. Tretiak, A. G. Pokrovsky, O. I. Kiselev , N. F. Salakhutdinov, *Eur. J. Med. Chem.*, 2015, **105**, 263—273; DOI: 10.1016/j.ejmech.2015.10.010.
42. B. J. Crielaard, S. Van Der Wal, H. T. Le, A. T. L. Bode, T. Lammers, W. E. Hennink, R. M. Schiffelers, M. H. A. M. Fens, G. Storm, *Eur. J. Pharm. Sci.*, 2012, **45**, 429—435; DOI: 10.1016/j.ejps.2011.08.027.
43. Y. B. Malysheva, S. Combes, D. Allegro, V. Peyrot, P. Knochel, A. E. Gavryushin, A. Y. Fedorov, *Bioorg. Med. Chem.*, 2012, **20**, 4271—4278; DOI: 10.1016/j.bmc.2012.05.072.
44. S. Günther, P. Y. A. Reinke, Y. Fernández-García, J. Lieske, T. J. Lane, H. M. Ginn, F. H. M. Koua, C. Ehrt, W. Ewert, D. Oberthuer, O. Yefanov, S. Meier, K. Lorenzen, B. Krichel, J.-D. Kopicki, L. Gelisio, W. Brehm, I. Dunkel, B. Seychell, H. Gieseler, B. Norton-Baker, B. Escudero-Pérez, M. Domaracky, S. Saouane, A. Tolstikova, T. A. White, A. Hänle, M. Groessler, H. Fleckenstein, F. Trost, M. Galchenkova, Y. Gevorkov, C. Li, S. Awel, A. Peck, M. Barthelmess, F. Schlünzen, P. Lourdu Xavier, N. Werner, H. Andaleeb, N. Ullah, S. Falke, V. Srinivasan, B. A. França, M. Schwinzer, H. Brognaro, C. Rogers, D. Melo, J. J. Zaitseva-Doyle, J. Knoska, G. E. Peña-Murillo, A. R. Mashhour, V. Hennicke, P. Fischer, J. Hakanpää, J. Meyer, P. Gribbon, B. Ellinger, M. Kuzikov, M. Wolf,

A. R. Beccari, G. Bourenkov, D. von Stetten, G. Pompidor, I. Bento, S. Panneerselvam, I. Karpics, T. R. Schneider, M. M. Garcia-Alai, S. Niebling, C. Günther, C. Schmidt, R. Schubert, H. Han, J. Boger, D. C. F. Monteiro, L. Zhang, X. Sun, J. Pletzer-Zelgert, J. Wollenhaupt, C. G. Feiler, M. S. Weiss, E.-C. Schulz, P. Mehrabi, K. Karničar, A. Usenik, J. Loboda, H. Tidow, A. Chari, R. Hilgenfeld, C. Uetrecht, R. Cox, A. Zaliani, T. Beck, M. Rarey, S. Günther, D. Turk, W. Hinrichs, H. N. Chapman, A. R. Pearson, C. Betzel, A. Meents, *Science*, 2021, **372**, 642—646; DOI: 10.1126/science.abf7945.

45. N. Drayman, J. K. DeMarco, K. A. Jones, S.-A. Azizi, H. M. Froggatt, K. Tan, N. I. Maltseva, S. Chen, V. Nicolaescu, S. Dvorkin, K. Furlong, R. S. Kathayat, M. R. Firpo, V. Mastrodomenico, E. A. Bruce, M. M. Schmidt, R. Jedrzejczak, M. Á. Muñoz-Alía, B. Schuster, V. Nair, K. Han, A. O´Brien, A. Tomatsidou, B. Meyer, M. Vignuzzi, D. Missiakas, J. W. Botten, C. B. Brooke, H. Lee, S. C. Baker, B. C. Mounce, N. S. Heaton, W. E. Severson, K. E. Palmer, B. C. Dickinson, A. Joachimiak, G. Randall, S. Tay, *Science*, 2021, **373**, 931—936; DOI: 10.1126/science.abg5827.
46. A. Clyde, S. Galanie, D. W. Kneller, H. Ma, Y. Babuji, B. Blaiszik, A. Brace, T. Brettin, K. Chard, R. Chard, L. Coates, I. Foster, D. Hauner, V. Kertesz, N. Kumar, H. Lee, Z. Li, A. Merzky, J. G. Schmidt, L. Tan, M. Titov, A. Trifan, M. Turilli, H. Van Dam, S. C. Chennubhotla, S. Jha, A. Kovalevsky, A. Ramanathan, M. S. Head, R. Stevens, *J. Chem. Inf. Model.*, 2022, **62**, 116—128; DOI: 10.1021/acs.jcim.1c00851.
47. G. J. Lockbaum, A. C. Reyes, J. M. Lee, R. Tilvawala, E. A. Nalivaika, A. Ali, N. Kurt Yilmaz, P. R. Thompson, C. A. Schiffer, *Viruses*, 2021, **13**, 174; DOI: 10.3390/v13020174.
48. C.-H. Zhang, E. A. Stone, M. Deshmukh, J. A. Ippolito, M. M. Ghahremanpour, J. Tirado-Rives, K. A. Spasov, S. Zhang, Y. Takeo, S. N. Kudalkar, Z. Liang, F. Isaacs, B. Lindenbach, S. J. Miller, K. S. Anderson, W. L. Jorgensen, *ACS Cent. Sci.*, 2021, **7**, 467—475; DOI: 10.1021/acscentsci.1c00039.
49. A. S. Christensen, T. Kubař, Q. Cui, M. Elstner, *Chem. Rev.*, 2016, **116**, 5301—5337; DOI: 10.1021/acs.chemrev.5b00584.
50. A. A. Adeniyi, M. E. S. Soliman, *Drug Discovery Today*, 2017, **22**, 1216—1223; DOI: 10.1016/j.drudis.2017.06.012.
51. D. Shcherbakov, D. Baev, M. Kalinin, A. Dalinger, V. Chirkova, S. Belenkaya, A. Khvostov, D. Krut´ko, A. Medved´ko, E. Volosnikova, E. Sharlaeva, D. Shanshin, T. Tolstikova, O. Yarovaya, R. Maksyutov, N. Salakhutdinov, S. Vatsadze, *ACS Med. Chem. Lett.*, 2022, **13**, 140—147; DOI: 10.1021/acsmedchemlett.1c00299.
52. C. Ma, Y. Hu, J. A. Townsend, P. I. Lagarias, M. T. Marty, A. Kolocouris, J. Wang, *ACS Pharmacol. Transl. Sci.*, 2020, **3**, 1265—1277; DOI: 10.1021/acsptsci.0c00130.
53. *Schrodinger Small Molecule Drug Discovery Suite*, Schrodinger, LLC, New York, NY, USA, 2017.
54. E. Harder, W. Damm, J. Maple, C. Wu, M. Reboul, J. Y. Xiang, L. Wang, D. Lupyan, M. K. Dahlgren, J. L. Knight, J. W. Kaus, D. S. Cerutti, G. Krilov, W. L. Jorgensen, R. Abel, R. A. Friesner, *J. Chem. Theory Comput.*, 2016, **12**, 281—296; DOI: 10.1021/acs.jctc.5b00864.
55. R. A. Friesner, R. B. Murphy, M. P. Repasky, L. L. Frye, J. R. Greenwood, T. A. Halgren, P. C. Sanschagrin, D. T. Mainz, *J. Med. Chem.*, 2006, **49**, 6177—6196; DOI: 10.1021/jm051256o.
56. W. Sherman, T. Day, M. P. Jacobson, R. A. Friesner, R. Farid, *J. Med. Chem.*, 2006, **49**, 534—553; DOI: 10.1021/jm050540c.
57. S. Genheden, U. Ryde, *Expert Opin. Drug Discovery*, 2015, **10**, 449—461; DOI: 10.1517/17460441.2015.1032936.
58. M. P. Jacobson, D. L. Pincus, C. S. Rapp, T. J. F. Day, B. Honig, D. E. Shaw, R. A. Friesner, *Proteins*: *Struct.*, *Funct.*, *Bioinf.*, 2004, **55**, 351—367; DOI: 10.1002/prot.10613.
59. R. W. Hockney, S. P. Goel, J. W. Eastwood, *J. Comput. Phys.*, 1974, **14**, 148—158; DOI: 10.1016/0021-9991(74)90010-2.
60. J. J. Stewart, *MOPAC 2016*, 2016.
61. A. Klamt, G. Schüürmann, *J. Chem. Soc.*, *Perkin Trans. 2*, 1993, 799—805; DOI: 10.1039/P29930000799.
62. J. Řezáč, P. Hobza, *J. Chem. Theory Comput.*, 2012, **8**, 141—151; DOI: 10.1021/ct200751e.
63. J. C. Phillips, R. Braun, W. Wang, J. Gumbart, E. Tajkhorshid, E. Villa, C. Chipot, R. D. Skeel, L. Kalé, K. Schulten, *J. Comput. Chem.*, 2005, **26**, 1781—1802; DOI: 10.1002/jcc.20289.
64. V. Zoete, M. A. Cuendet, A. Grosdidier, O. Michielin, *J. Comput. Chem.*, 2011, **32**, 2359—2368; DOI: 10.1002/jcc.21816.
65. A. D. MacKerell, D. Bashford, M. Bellott, R. L. Dunbrack, J. D. Evanseck, M. J. Field, S. Fischer, J. Gao, H. Guo, S. Ha, D. Joseph-McCarthy, L. Kuchnir, K. Kuczera, F. T. K. Lau, C. Mattos, S. Michnick, T. Ngo, D. T. Nguyen, B. Prodhom, W. E. Reiher, B. Roux, M. Schlenkrich, J. C. Smith, R. Stote, J. Straub, M. Watanabe, J. Wiórkiewicz-Kuczera, D. Yin, M. Karplus, *J. Phys. Chem. B*, 1998, **102**, 3586—3616; DOI: 10.1021/jp973084f.
66. W. Humphrey, A. Dalke, K. Schulten, *J. Mol. Graph.*, 1996, **14**, 33—38; DOI: 10.1016/0263-7855(96)00018-5.
67. H. Attouch, R. Cominetti, *J. Differ. Equ.*, 1996, **128**, 519—540; DOI: 10.1006/jdeq.1996.0104.
68. A. Pedretti, A. Mazzolari, S. Gervasoni, L. Fumagalli, G. Vistoli, *Bioinformatics*, 2021, **37**, 1174—1175; DOI: 10.1093/bioinformatics/btaa774.

Received April 28, 2022;
in revised form May 19, 2022;
accepted May 25, 2022